A Strain Energy Based Criterion for Multiaxial Fatigue Failure

Fernand Ellyin [1]

[1] Department of Materials Engineering, The University of British Columbia, Vancouver, B.C. Canada V6T 1Z4, e-mail: fernand@comopsites.ubc.ca

Abstract. Research on the fatigue resistance of mechanical components / structures has been proceeding for nearly a century and half. Yet, there is no universally agreed upon damage criterion which can predict most aspects of fatigue failure. The reason is the complexity of phenomenon and its dependence on the microstructure. Here, we present a strain energy based damage parameter which has an underlying microscopic basis. A master life curve is subsequently defined which correlates well with the experimental data of two classes of materials: metals and metal matrix composites.

INTRODUCTION

A majority of mechanical / structural components are subjected to multiaxial stress states. Even if the applied load is uniaxial, stresses at notch roots or geometric discontinuities would be multiaxial. Residual stresses introduced during manufacturing process, could also be multiaxial due to temperature gradient. Indeed the early published investigations on fatigue resistance were on shafts of rotating machines where bending and torsion couples were applied to simulate service loads [1]. These investigations were mostly of an empirical nature and were generally concerned with finding design formulae for long-life cyclic loading of machine components. A drawback of these types of investigations was that their range of application was limited to the scope of the experimental data.

Studies on fatigue mechanisms did not begin in earnest until the complete formulation of linear elastic (mid-fifties) and non-linear fracture mechanics in late sixties. However, despite nearly a century and half of efforts expanded on the subject, there is no universally agreed upon theory that can predict most aspects of fatigue failure. The reason is, to some extent, the complexity of phenomenon and its dependence on the micro-structural variables. Any macroscopic fatigue damage parameter / function must have an underlying microscopic basis, since damage invariably initiates at this scale.

OBSERVATIONS ON THE SURFACE

Investigations on the fatigue mechanisms mostly have focused on single crystals (e.g. copper) to obtain fundamental features of crack nucleation, initiation and propagation. These studies have indicated that the deformation

process is comprised of two stages. In the early stage of rapid strain hardening, the deformation is almost homogeneous and surface markings are fine and uniformly distributed. Following cyclic saturation, persistent slip bands (PSBs) are formed with rough profiles of extrusion and intrusions.

In polycrystals the PSBs are generally formed in the surface grains which have suitable orientation for slips to occur. In the case of copper polycrystals, the extrusion effect is much smaller than that of the single crystal. Figure 1 is a schematic illustration of slip formations during cyclic loading leading to extrusions and intrusions. It is worthwhile to mention that slip bands are major sites of crack initiation, and that the plastic strain in the PSB lamellae is at least an order of magnitude higher than that in the matrix (see ref. [2] for further discussion).

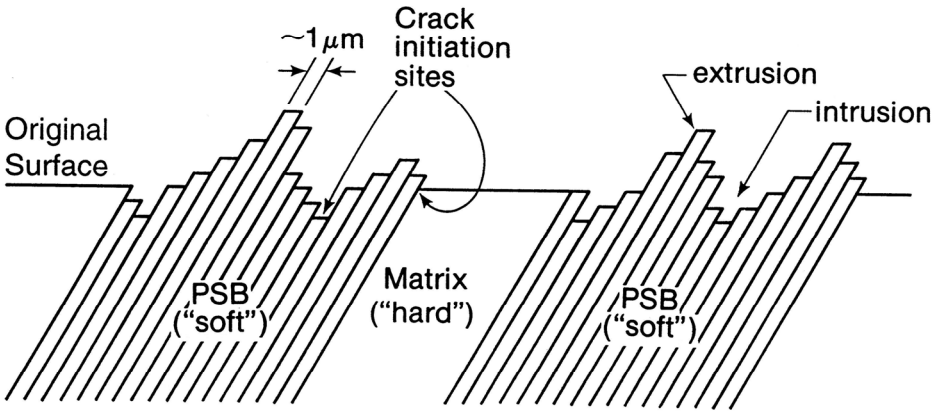

Figure 1. Schematic of slip profile during cyclic loading in polycrystals [2].

Influence of Stress State on the Surface

To understand the influence of multiaxial stresses on the fatigue process, a material element near the surface is isolated as shown in Fig. 2. The stresses acting on the element are: pure shear, uniaxial and equi-biaxial. First let us define what is implied by a "multiaxial" stress state. When a bar of uniform cross-section is subjected to an axial load, at sections inclined to the applied load ($0° < \theta < 90°$) two stress components, one normal and the other tangential to the cross-section will be present. Therefore, a multiaxial stress state in a fatigue analysis must be defined with respect to the principal stress components. Thus, with reference to Fig. 2, the pure shear is multiaxial, comprised of two principal stresses acting on the element with equal magnitude but of opposite sign. Note that the other two stress states in Fig. 2 are obtained by adding a tensile stress component in the transverse direction, $\sigma_2 = \sigma_1$, to

obtain uniaxial and equi-biaxial stress states. The corresponding maximum shear stress planes are also shown in Fig. 2.

Note that for a pure shear loading an initiated crack will propagate faster along the surface than through the thickness (principal direction 3), i.e. it will be a shallow crack. In the case of uniaxial loading an initiated crack would grow

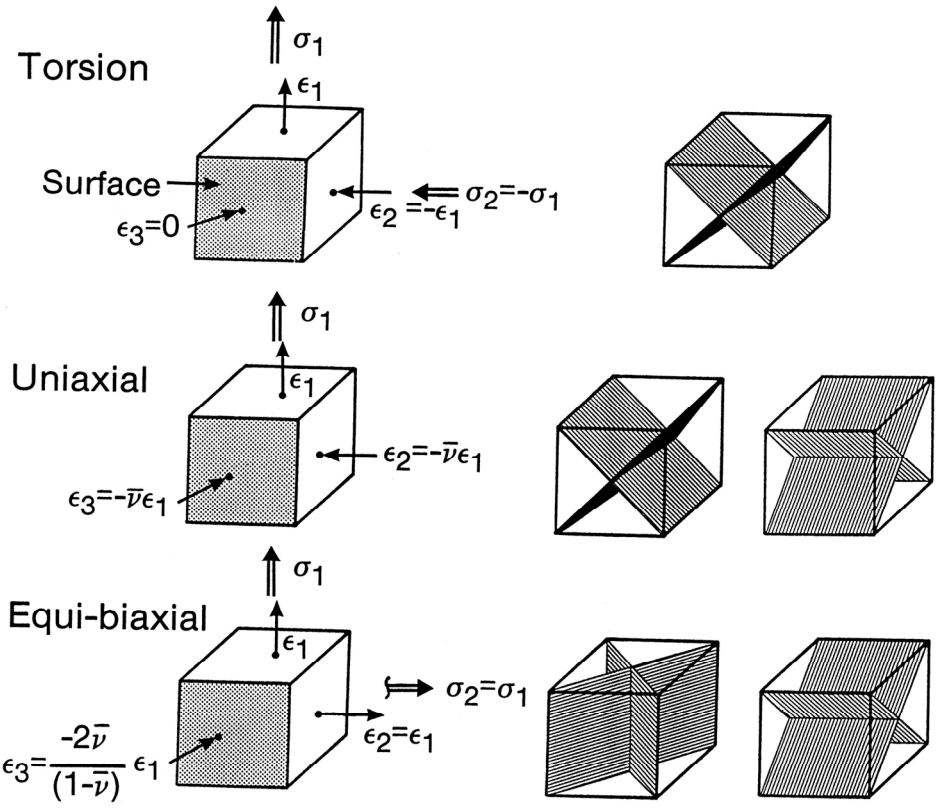

Figure 2. An element near the surface of a material subjected to shear, uniaxial and equi-biaxial loading; the corresponding strain states, and the maximum shear stress planes are depicted in the figure [2].

deeper into the material. The difference between the uniaxial and equi-biaxial stress states is that in the latter both pair of the maximum shear planes indicates crack initiation and growth into the material (away from the surface) resulting in deeper cracks. For the same applied equivalent stress, the fatigue life decreases as one moves down each stress state in Fig. 2, i.e. the pure shear will have the longest life and equi-biaxial the shortest fatigue life.

Multiaxial Constraint Factor (MCF)

Let us now examine the strain state for the applied stress states in Fig. 2. (Note that irrespective of the applied load, the strain state is three dimensional.) As shown in Fig. 2, the maximum shear strain, $\hat{\gamma}$, in a direction inclined $45°$ to the surface is important in the initiation of cracks (sliding mode). Similarly, the maximum in-plane principal strain, $\hat{\varepsilon}$, affects the crack propagation (opening mode). Thus, these two strains define the surface condition for crack initiation and growth.

It has been shown in [2] that by defining an appropriate constraint factor, the multiaxial fatigue data for various combinations of imposed strain ratios and loading paths can be reduced to a unique (master) life curve.

The multiaxial constraint factor (MCF) is defined by:

$$\overline{\rho} = (1-\overline{\upsilon})\frac{\hat{\varepsilon}}{\hat{\gamma}} \tag{1}$$

where

$$\begin{aligned} \hat{\varepsilon} &= \max\left[\varepsilon_a \text{ or } \varepsilon_t\right] \\ \hat{\gamma} &= \max\left[\left|\varepsilon_a - \varepsilon_r\right| \text{ or } \left|\varepsilon_t - \varepsilon_r\right|\right] \end{aligned} \tag{2}$$

$\overline{\upsilon}$ is an effective Poisson's ratio, bounded between the elastic and plastic values. In the above ε_a and ε_t are the peak values of principal strain components (axial and transversal) on the planes parallel to the surface. ε_r is perpendicular to the surface [2],

$$\varepsilon_r = \frac{-\overline{\upsilon}}{1-\overline{\upsilon}}(\varepsilon_a + \varepsilon_t) \tag{3}$$

The MCF defined by Eq.1 plays an important role in defining the fatigue damage process. In the case of fully reversed cyclic shear loading ($\varepsilon_a = -\varepsilon_t$), $\overline{\rho} = 1+\overline{\upsilon}$; for uniaxial loading ($\varepsilon_r = \varepsilon_t = -\overline{\upsilon}\varepsilon_a$), $\overline{\rho} = 1$ and for equi-biaxial loading ($\varepsilon_a = \varepsilon_t$), $\overline{\rho} = 1-\overline{\upsilon}$. Thus, $1/\overline{\rho}$ indicates the severity of a particular loading with reference to the uniaxial stress condition.

For an out-of-phase (non-proportional) loading, the value of $\overline{\rho}$ changes with time and its derivation can be found in ref. [2].

MULTIAXIAL FATIGUE DAMAGE PARAMETER

From the metallographic studies of metals discussed earlier, it is clear that PSBs form as a result of strain localization, and cracks initiate anywhere within

or near the interface of PSBs. Since neither the applied stress nor strain can be directly related to the stress / strain fields in and near the PSBs, the only plausible parameter is the strain energy in the surrounding matrix which constrains the PSB lamellae deformation.

The suitability of the strain energy as a damage parameter can also be shown using the first law of thermodynamics, see refs. [2, 3], that indicates that the damage energy is related to the inelastic strain energy.

The inelastic (or plastic) energy per cycle, ΔW^p, is determined from

$$\Delta W^p = \int_{cycle} \sigma_{ij} d\varepsilon_{ij}^p \qquad (i,\ j = 1,\ 2,\ 3) \tag{4}$$

And the multiaxial damage parameter is then defined by:

$$\Psi_p = \Delta W^p / \overline{\rho} \tag{5}$$

where $\overline{\rho}$ is given by Eq. 1. To carry out the integration in (4) one would require a constitutive relation for the inelastic cyclic deformation. (For example, see Ellyin [2] Chapter 6 for a discussion of appropriate constitutive models.)

In high-cycle (low strain) fatigue, the damage process associated with the plastic deformation occurs in localized regions on a micro (grain size) scale. The macroscopic (bulk) response of the material is essentially elastic, i.e. $\Delta W^p \approx 0$. Note also that the elastic strain energy per cycle is recovered, i.e. $\Delta W^e = 0$. However, experimental studies have indicated that superposed hydrostatic tension decreases the fatigue life, while hydrostatic compression increases it. Thus, in contrast to the yielding of metals and alloys, the effect of the hydrostatic pressure has to be accounted for in fatigue damage. To account for the above, it has been proposed [2, 3] that the elastic energy associated with the tensile stress, ΔW^{e+}, be included in the damage parameter Eq. 5. This part of energy during a cycle is calculated from

$$\Delta W^{e+} = \int_{t}^{t+T} H(\sigma_i) H(d\varepsilon_i^e) \sigma_i d\varepsilon_i^e \qquad (i = 1,\ 2,\ 3) \tag{6}$$

where *T* is the period of the cycle, σ_i is a principal stress component and $H(x)$ is the Heaviside function, equal to unity for $x \geq 0$ and zero when $x < 0$.

A damage function applicable to both high- and low-cycle fatigue is then obtained by adding Eqs. 5 and 6, noting that the energy is a scalar quantity,

$$\Psi = [\Delta W^p / \overline{\rho} + \Delta W^{e+}] \tag{7}$$

A single curve (master curve) for all stress states is obtained by equating Eq. 7 to number of cycles to failure, N_f. The master life curve has the form of,

$$(\Delta W^p / \overline{\rho}) + \Delta W^{e+} = \kappa (N_f)^{\alpha} + C \tag{8}$$

where, $\kappa > 0$, $\alpha < 0$, and $C \geq 0$ are material constants to be determined from appropriate tests. The left-hand-side of Eq. 8 is the crack driving energy. The constant *C* on the right-hand-side (RHS) of Eq. 8 is the non-damaging energy associated with the fatigue limit of the material. If the material does not exhibit a fatigue limit, then $C = 0$.

The constants on the RHS of Eq. 8 can be determined by performing uniaxial tests in which $\overline{\rho} = 1$ and finding the constant through a best fit procedure. Once the constants are determined, then the master curve, Eq. 8 can be written as (subscript 'u' in Eq. 9 refers to the uniaxial loading),

$$\Psi = (\Delta W^p / \overline{\rho}) + \Delta W^{e+} = \kappa_u (N_f)^{\alpha_u} + C_u \tag{9}$$

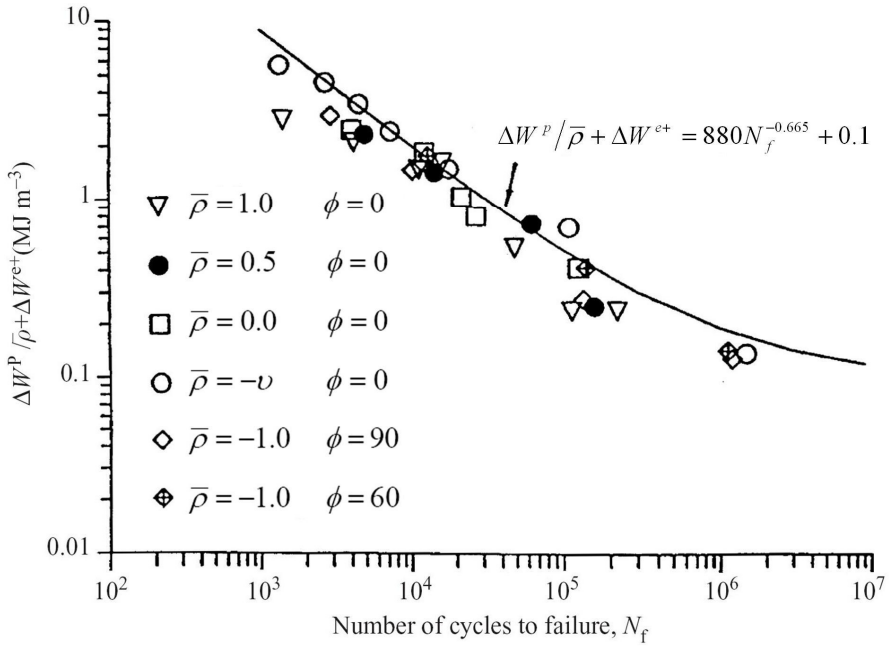

Figure 3. A log-log plot of the driving strain energy per cycle versus number of cycles to failure and correlation with the multiaxial experimental data of low alloy steel ASTM A516 Gr. 70

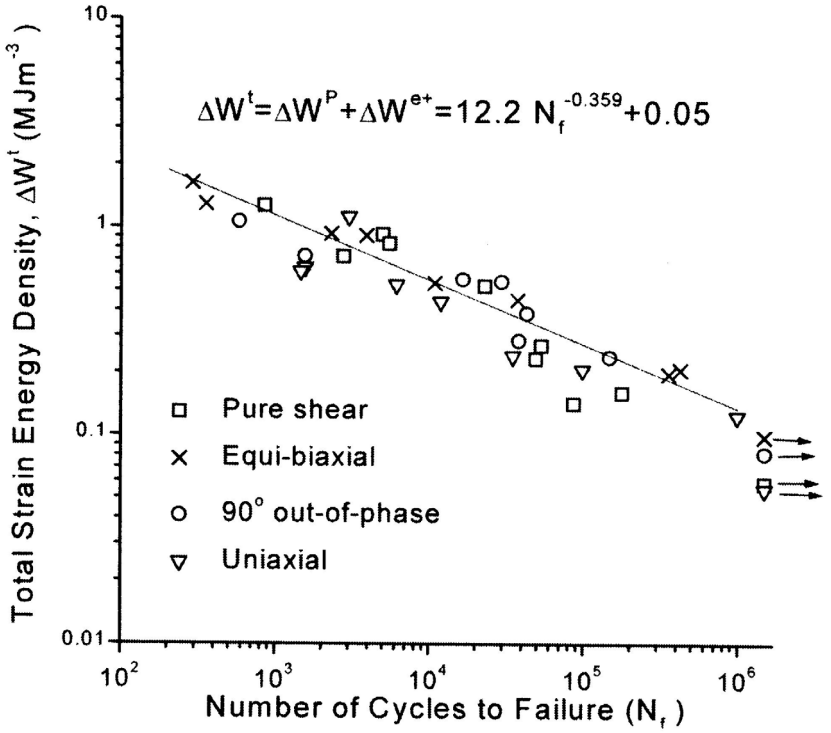

Figure 4. A log-log plot of the driving strain energy per cycle versus number of cycles to failure and correlation with the multiaxial experimental data: metal matrix composite Al_2O_3 / 6061 Al.

COMPARISON WITH EXPERIMENTAL DATA

In this section we will compare the prediction of Eq. 9 with test data of two types of materials. One is a low-alloy steel designated as ASTM A516 Gr. 70. The second is a metal matrix composite, alumina particle reinforced aluminum alloy, Al_2O_3 / 6061 Al.

All tests were conducted on thin-walled tubular specimens subjected to fluctuating axial force and through-wall differential pressure (constant exterior pressure and fluctuating internal pressure). The tests were conducted under fully reversed strain-control with varying in-plane strain ratio, $\rho = \Delta\varepsilon_t / \Delta\varepsilon_a$, and phase angle ϕ.

Figure 3 shows the damage parameter,ψ, LHS of Eq. 9 versus the number of cycles to failures, N_f in a log-log scale. Also plotted in Fig.3 is Eq. 9. It is seen that the agreement is very good.

In Fig. 4, 36 test data are plotted in a log-log coordinate system [4]. Both proportional and non-proportional strain paths are included. Here too it is noted

that the total strain energy density criterion correlates very well with the test results of four types of loading paths by a unique strain energy- fatigue life curve (master life curve).

Lazzarin and Berto [5] recently have shown the applicability of Eq. 9 to notched components.

CONCLUSIONS

A damage parameter for multiaxial stress states is proposed which is comprised of plastic energy per cycle, ΔW^p, normalized with respect to the multiaxial constraint factor on the surface of a homogeneous material, $\overline{\rho}$, and the elastic tensile strain energy per cycle, ΔW^{e+}. A fatigue criterion is then obtained by correlating the driving energy ($\Delta W^p / \overline{\rho} + \Delta W^{e+}$) to the number of cycles to failure N_f to produce a master life curve. The predicted results are found to be in very good agreement with the experimental results of multiaxial loading for two very different material systems.

For the sake of compactness, the discussion in this paper has been focused on fully reversed multiaxial loading. The effect of the mean stress and racheting strain, and time-dependent fatigue (creep-fatigue interaction) were not discussed. These can be found in the references listed below.

REFERENCES

1. Lanza, G. (1886) *Trans. ASME*. **8,** 130-134.
2. Ellyin, F. (1997) *Fatigue Damage, Crack Growth and Life Prediction*. Chapman and Hall, London, UK
3. Ellyin, F. (2001), in: *Encyclopedia of Materials: Science and Technology*, pp. 2939-2944, Elsevier Science Ltd., Amsterdam, the Netherlands .
4. Xia, Z. and Ellyin, F. (1998) *Int. J. Fatigue* **20**, 51-56.
5. Lazzarin, P. and Berto, F. (2008) *Fatigue Fract Engng Mater Struct*. **31**, 95-107.